COMPUTATIONAL FLUID DYNAMICS ANALYSIS OF ISOTHERMAL AND NON-ISOTHERMAL TWIN JETS

A Thesis

by

MOHAMMAD TAREQ HUSSEIN BANI AHMAD

Submitted to the Office of Graduate and Professional Studies of
Texas A&M University
in partial fulfillment of the requirements for the degree of

MASTER OF SCIENCE

Chair of Committee,	Yassin Hassan
Co-Chair of Committee,	Rodolfo Vaghetto
Committee Members,	Maria King
Head of Department,	Yassin Hassan

December 2017

Major Subject: Nuclear Engineering

ABSTRACT

This study has been conducted in a partial fulfillment of a master of science degree in nuclear engineering from the department of nuclear engineering at Texas A&M University (TAMU).

The study aims to perform a computational fluid dynamics analysis using the commercial software package STAR-CCM+ to compare the behavior of twin jets with equal velocities under isothermal (same temperature) and non-isothermal (different temperature) flows. The behavior of twin jets has a very wide range of application in engineering, from combustion chambers and fuel injectors, to fighter jets and sodium-cooled reactors.

This study investigates the twin jets that were constructed by The University of Tennessee at Knoxville (UTK) and are located at the TAMU thermal hydraulics lab. This work was performed to gain a better understanding of the difference between isothermal and non-isothermal flows as this will provide better judgment to the safety analysis of future design reactors. The temperature difference in non-isothermal flows has been seen to affect some flow properties in this study.

CONTRIBUTORS AND FUNDING SOURCES

Contributors

This work was supported by a thesis committee consisting of Professor Yassin Hassan (advisor) and Professor Rodolfo Vaghetto of the Department of Nuclear Engineering. Professor Maria King of the Department of Biological and Agricultural Engineering. The work done for this thesis was completed by the student, under the advisement of Professor Yassin Hassan of the Department of Nuclear Engineering.

Funding Sources

This research was supported by a teaching assistantship by the Department of Nuclear Engineering at Texas A&M University.

TABLE OF CONTENTS

LIST OF FIGURES

LIST OF TABLES

Page

1. INTRODUCTION

Computational Fluid Dynamics (CFD) is the science of using applied mathematics and physics through computational software to visualize how fluids flow and/or interact with structures while flowing. CFD uses the Navier-Stokes equation to describe how the velocity, pressure, temperature, and density of a fluid in motion are related. In the past decades interest in using CFD simulation has been growing intensively. As CFD uses numerical schemes to solve the Navier-Stokes, inaccuracies are inevitable, which makes the accurate prediction of the flow behavior and the capturing of the associated physics challenging.

Twin jets are an important shear flow that is involved in many industrial applications. From airplanes, combustions engines to Generation IV nuclear reactors. In Generation IV reactors the coolants merge in the upper or lower plenum after passing through the reactor core. The temperature differences in the reactors plenums may induce flow vibrations, thermal stratification, buoyancy driven flows, and other phenomena that may cause thermal stresses and fatigues, which will threaten the core structure and cause safety related concerns. Thus, the thorough mixing induced by turbulent jets is a very important aspect of nuclear thermal hydraulics that must be studied carefully and analyzed accurately.

2. WHY TWIN JETS?

Generation IV reactors are a set of nuclear reactors designs that are currently being researched for commercial purposes. Of these reactor designs are the Liquid Metal Cooled Fast Reactors (LMFR) and the Very High Temperature Reactors (VHTR). These reactors are motivated by the enhancement of nuclear reactors safety, economy, efficiency, and sustainability.

Many challenges are facing the commercialization of these reactor designs and many of these challenges are safety related. The reactor core is the area in which the nuclear fuel is located, this area requires large amounts of continuous cooling. The continuous water feed to the core takes the heat generated by the fuel to the upper plenum which lies above the core outlet. The upper plenum supports the control rods and the instrumentation above the core. The coolant coming from the core at high velocity a long with radial flow may induce vibrations. Detailed calculations are necessary to determine the risk of flow induced vibrations. Along with the presence of the vibrations are the temperature oscillations that occur due to different temperature gradients, this will potentially cause thermal fatigue which will threaten the core integrity and lead to a severe accident. Thermal fatigue can also be caused by the gas entrainment in the upper plenum after it has been thermally stratified. Also, with transient scenarios, and a decrease in mass flow rate, buoyancy forces may have negative effect on the flow that will lead to thermal fatigue. Figure 1 shows the challenges associated with the upper plenum (Tenchine, 2010).

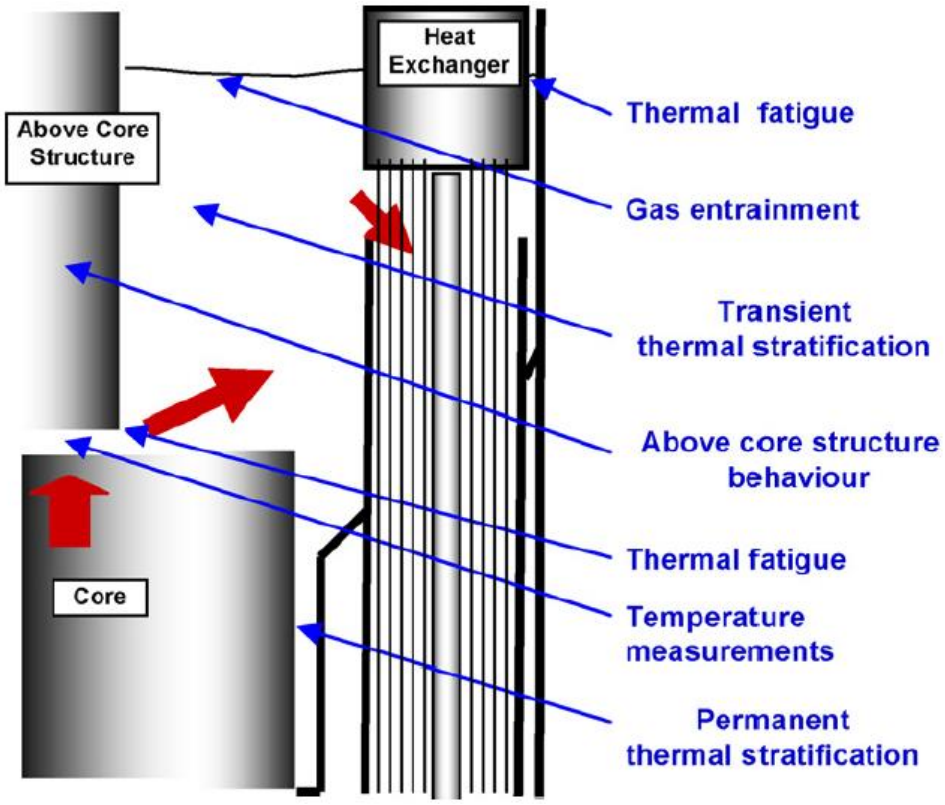

Figure 1: Reactor Upper Plenum and Associated Challenges (Tenchine, 2010).

Thermal stripping is a phenomena that occurs in an environment where cold and hot fluids are mixed. The thermal fatigue process can be divided into five processes (Kimura, Miyakoshi and Kamide, 2007):

1- The presence of temperature fluctuation due to the convective mixing between hot and cold fluids.

2- Attenuation of temperature fluctuation in the boundary layer near the structure.

3- Heat transfer between the fluid and the structure.

4- Thermal conduction in the structure.

5- Thermal fatigue in the structure.

To overcome these challenges accurate and valid calculations are needed, especially in environments or conditions where experiments are not feasible or viable. The use of CFD will provide great help in such tasks, and this will save time, money, and effort in analysis of the new generation reactors.

3. LITERATURE REVIEW

Twin jets was first brought to investigation back in 1959 when Miller and comings (David and Edward, 1959) measured the mean velocity, mean flow direction, normal turbulent stress in the direction of flow, and mean static pressure for a subsonic flow field generated by identical twin jets of air with parallel slot nozzles. Tanaka [1, 2] have experimentally studied the entry point and the combined region of the twin jets and determined the distribution of the cavity pressure, mean and fluctuating velocities, shape of the jets and cavity length. Tanaka found out that two jets attract each other and the axis of a jet coincides with an arc of a circle. Also, the velocity flow profiles of the combined flow are similar and agree well with the theoretical profile of the single jet, but the distributions of the turbulence intensities shows a different behavior than that of a single jet. Marsters recorded experimental observations of the flow field of two plane, parallel jets as they merge into a stagnant surroundings (Marsters, 1977). Marsters compared the experimental results with predictions based on a simple momentum integral analysis of the flow field. The crude analysis predicted the merging of the jets reasonably well, but it failed to predict the secondary flow entrained in the unobstructed space between the jet nozzles.

Elbanna and Gahin studied the interaction of two-dimensional parallel jets, their measurements included mean velocity, turbulence intensities, and Reynolds shear stress. The structure of combined flow is then compared to that of a single jet and gave a good

agreement. They concluded that up to 120 slot widths downstream of the nozzle, true similarity was not found (Elbanna, Gahin And Rashed, 1983) . Elabanna and Sabbagh also studied the interaction of two none-equal pane parallel jets and have observed a negative static pressure upstream of the merging region, while the highest pressure was in the combination region (Elbanna and Sabbagh, 1987).

Ko studied the flow structures in the initial region of two parallel jets, their analysis included velocity measurements in the time and frequency domain and have found the inner and outer mixing region which have their own coherent structures, which are of vortical form (Ko and Lau, 1989). Lin and Sheu have used hot wire anemometer to investigate the flow field generated by two identical jets of air. They have found out that the mean velocity approaches self-preservation in both the converging and the combined regions, while the turbulent intensities and Reynolds shear stress approach self-preservation in the combined region only. Also, the trajectory of the of the maximum velocity is almost unchanged by variance of nozzle spacing in the converging region (Y. E. Lin and Sheu, 1990).

Lin and Sheu have studied the interaction of two plane parallel turbulent jets using a split-film probe on a constant temperature anemometer. They have measured mean velocities, mean flow directions, turbulent intensities, and the Reynolds shear stresses of the three main regions in the twin jets (Y. F. Lin and Sheu, 1990). Harpham and Shambaugh carried out an experimental investigation on the flow field of a two parallel, rectangular air nozzles. The nozzles had a large length to width ratio and the nozzles were closely spaced and intersected at an angle of 60º. They found out that near the center of

the nozzle, the flow field is estimated to that of a two dimensional jet. They have tested different jets with varying the slot widths and have developed correlations to predict the velocity at any position below the pair of nozzles (Harpham and Shambaugh, 1996). They also extended their previous work to nonisothermal jets and their operating temperature fields ranged from ambient to 321 ºC and have developed correlations to describe the temperature and velocity fields (Harpham and Shambaugh, 1997).

Lai and Nasr investigated the velocity field of two parallel plane jets experimentally and numerically using Laser Doppler Anemometry (LDA) and FLUENT software package, for the numerical simulation they have used three turbulence models, κ-ε, RNG κ-ε, and Reynold Stress to predict the flow field, the merging length varied by 18% between the experimental measurements and the simulation results, as for the jet spread and the outer shear layer, both were under predicted by three turbulence models (Lai and Nasr, 1998).

Anderson and Spall carried out an experimental and investigation of two-dimensional parallel jets using x-type hot-wire probe and the Reynolds Stress (RSM) and standard κ-ε turbulence models, for the numerical simulation the FLUENT software package was used. They found out that the numerical model predicted the merging and combined point characteristics accurately. The velocity field along the symmetry plane agrees well with experimental data, but the models show a narrower width of the jet spread than what is measured by the experiment (Anderson and Spall, 2001).

Grinstein investigated vortex dynamics entrainment in rectangular free jets numerically using Large Eddy Simulation (LES) for a compressible (subsonic) jets initialized with laminar conditions. Grinstein found out that the near field entrainment properties of a low aspect ratio rectangular jets are shown to be largely determined by the characteristic aspect ratio-dependent coupling geometry of interacting rib and ring vortices and by vortex-ring axis-switching times (Grinstein, 2001).

Spall carried out a numerical simulation to assess the influence of buoyancy on plane parallel jets, Spall used the software package FLUENT and the κ-ε turbulence model. Spall concluded that the merging point of the parallel jets, along the plane of symmetry, decreases with increasing of the jet temperature, he attributed that to the higher entrainment rates compared to the isothermal jets (Spall, 2002). Spall and Anderson studied the evolution of the streamwise momentum flux for two turbulent, plane, parallel plane jets numerically and experimentally, they used a standard κ-ε model for their turbulence model. They have measured the integral of the momentum flux downstream of the merging point. Numerical calculations of the integral constant found that the constant decreases as the jet spacing increases, and decreases as the jet entrainment rates increase due to higher levels of inlet turbulent kinetic energy, or, decreased levels of dissipation rate. Also, the streamwise distance towards the merge point was also found to decrease for higher levels of turbulent kinetic energy or lower levels of dissipation rate at the jet inlet (Spall, Anderson and Allen, 2004).

Sarit K. Das et al. investigated the interaction between two identical turbulent jets mixing with ambient air numerically to investigate the temperature and velocity

oscillations in the mixing zone. The analysis was carried out using the FLUENT software package. The spread angle was found to be slightly lower than that of a single jet. The analysis was carried out for Reynolds numbers that range from 9000-12000 and a non-dimensional nozzle spacing 30 and 40. The results of the simulation were validated with experimental data. Their results show that the regular periodic oscillations occur at low Reynolds number with a single dominant frequency. These oscillations were found to change to a non-periodic form as the Reynolds number is increased as flow is transitioning to a turbulent flow (Suyambazhahan, Das and Sundararajan, 2004).

Das et al. also extended their work to include non-isothermal twin parallel jets in horizontal orientation numerically to ascertain the mean flow structure and oscillation characteristics of temperature and velocity fields. The analysis was carried for and Reynolds number between 9000-12000 and a Grashof number range between 50 and 100, they used the FLUENT software package and their results compare well with experimental data. Their results concluded that buoyancy has considerable influence on the jet flow oscillation characteristics as well as the recirculation zones and the merging point between the jets. In the interacting shear layers, the frequency of oscillations decreases and amplitude increases, with nozzle spacing. Also, the frequency of the oscillations increases first and then decreases with respect to the jet inlet temperature. And as for the amplitude of the oscillations, it increases with the increase of inlet temperature (Suyambazhahan, Das and Sundararajan, 2007). Das et al also investigated low speed laminar horizontal parallel jets experimentally and theoretically. For the numerical analysis the FLUENT software package was used. They concluded that buoyancy has a significant effect on the

local velocity fluctuations and convective instabilities for a forced convection dominated flow. The dominant frequency and the amplitude of velocity fluctuations depend on the exit temperature and spatial location within the jet. For isothermal jets, the dominant frequency of the oscillation shows a linear behavior with the Reynolds number, for the nonisothermal jets, it shows a non-linearity with the Reynolds number (Suyambazhahan, Das and Sundararajan, 2009).

Durve et al carried out a numerical investigation on twin and triple jets, they used FLUENT software package in their study. They used the Reynolds stress model for turbulence modeling. The results predicted by the Reynolds stress model agree well with the experimental data of axial velocity and shear stress. Results were compared with the single jet to observe the effect of adding a jet on the mixing phenomena and turbulent fluctuations. (Durve *et al.*, 2012).

Carasik et al carried out a numerical simulation on isothermal twin jets using STAR-CCM+ software package, they used realizable κ-ε as their turbulence model. Their results agree well with experimental data (L. B. Carasik, A. E. Ruggles2, 2014). Hnaien carried out a numerical investigation on the interaction of parallel jets. They used the standard κ-ε, the standard κ-ω, and the RSM turbulence models. Their investigation shows that increasing the velocity ratio between the jets raises the merging and combining points further upstream as the weaker jet is attracted to the faster jet (Hnaien *et al.*, 2016).

Wang et al. used Laser-Doppler Anemometry to evaluate the mixing characteristics of equal (same velocity) turbulent isothermal jets. They measured the

turbulent characteristics such as mean velocities, turbulence intensities, Reynolds Stresses, and z component vorticities (Wang *et al.*, 2016). They also did Particle Imaging Velocimetry (PIV) for the same that twin jets, and the results of PIV and LDV agree well (Wang, Lee and Hassan, 2016).

4. PHYSICS OF TWIN JETS

The flow structure of a parallel rectangular jet can be divided into three regions; the converging region, merging region, and the combined region.

1) The converging region is the region between the jets outlet and merging point (MP). The merging point is the point at which the streamwise velocity is equal to zero.
2) The merging region is the region between the MP and combining point (CP). The combining point is the point is the point where the streamwise velocity is maximum.
3) The combined region is the region beyond the CP and this region is characterized by the development of both jets and forming one jet.

The entrainment of the two jets in the converging region causes the jets to deflect and form a recirculating region. The velocity of the jets creates a sub-atmospheric region characterized by negative pressure. This region exists near the inlet and causes the jets to become attracted to each other and combine to form a single jet. The flow structures of the jet are shown in Figure 2.

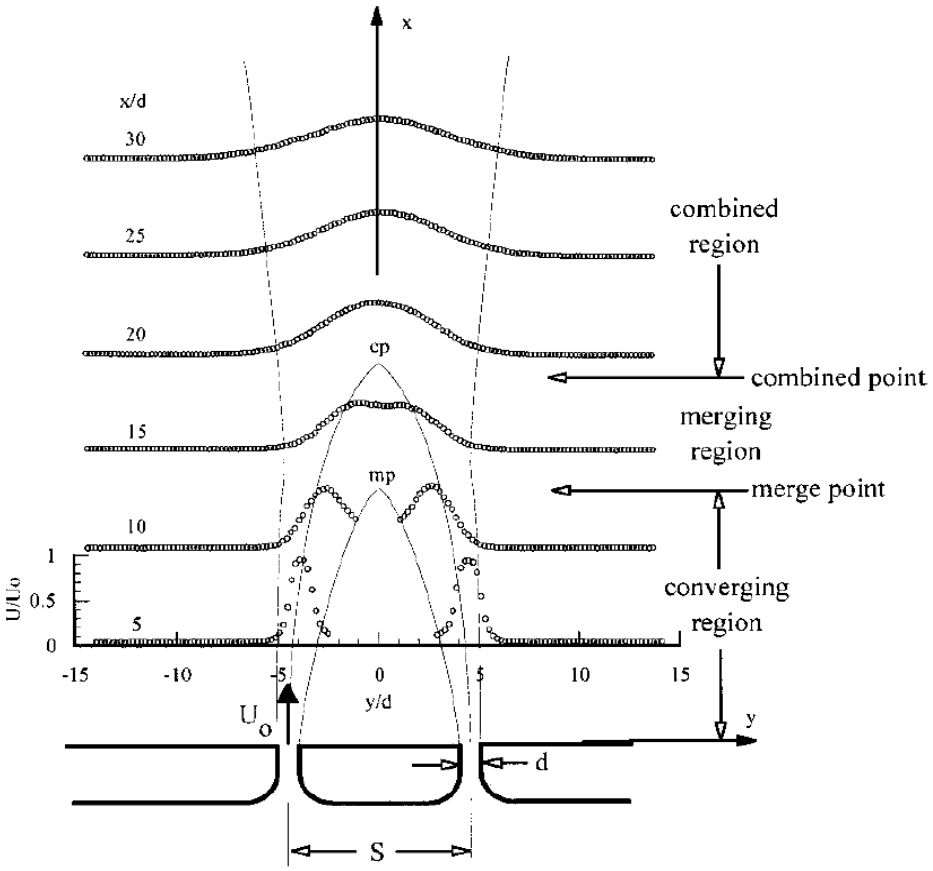

Figure 2: The Flow Structures Associated With Twin Jets.

5. EXPERIMENTAL FACILITY

This section is dedicated to demonstrate the Twin Jet Water Facility constructed at the University of Tennessee at Knoxville. The facility is located the Thermal Hydraulics LAB at Texas A&M University. The setup is shown in Figure 3. The facility consists of an acrylic tank (to provide optical access) with a capacity of 0.76 m^3. Located at the center of the tank are two nozzles so the jets can develop freely without any effect from the lateral walls. Beneath the jets are stagnation boxes that are present to remove any undesired fluctuations in the flow. To the back of the tank are two overflow plates that redirect the flow into two reservoirs that are under the tank. The two tanks are separated to ensure the two fluid flows coming to both nozzles don't interact with each other, which is very important for this case as the nozzles carry fluids that have the same velocity but are at a different temperature. The water then leaves the tank through the overflow plates and is then are recirculated to the reservoirs under the tank. The height of the nozzles is sufficient long to ensure a developed turbulent velocity profile and the thickness of the walls of the tank 25.4 mm. [3]

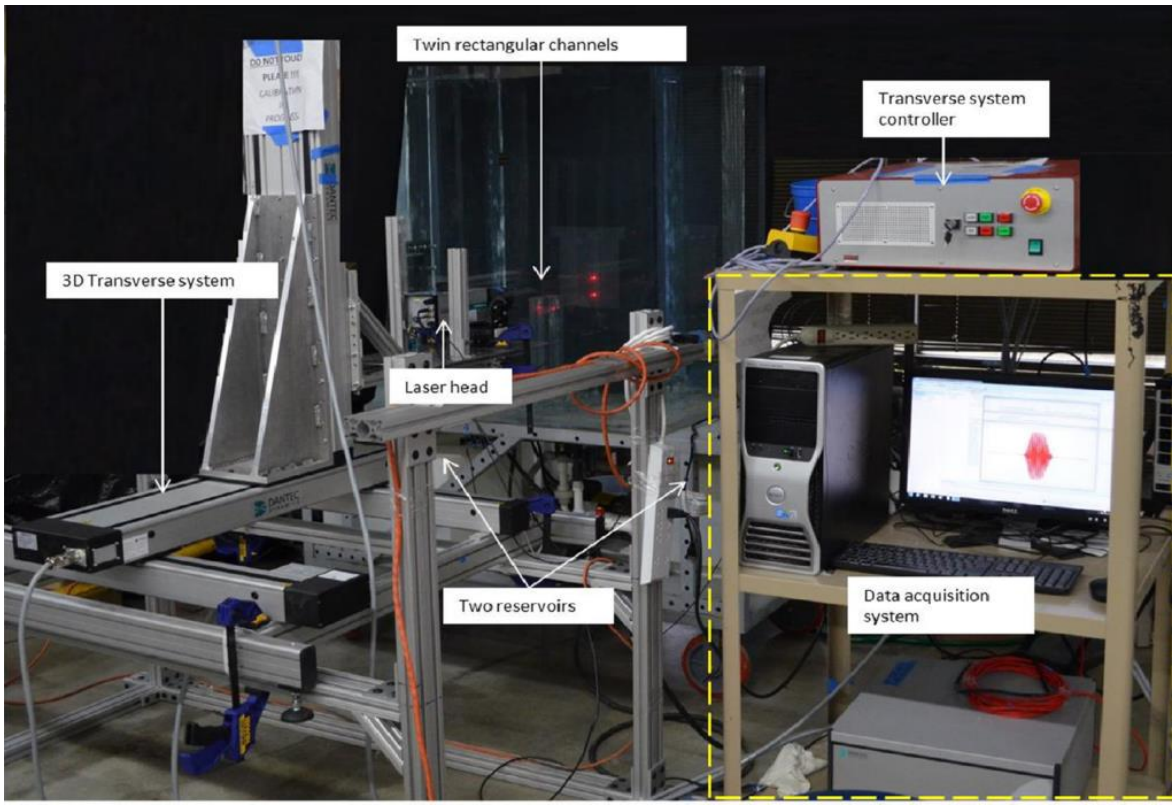

Figure 3: Twin Jet Facility [3].

The nozzle flow was driven by two 373 watt pumps. The control of the two jets were independent. The flow meter used is GPI TM100 with an accuracy of 97% and repeatability of 95%. The facility is able to operate as single and dual jet. The rectangular nozzles have a width of a = 5.8 mm and length 87.6 mm, the spacing between the centerline of the two nozzles is of s = 17.8 mm. the height of the nozzles slot is 279.4 mm. Figures 4,5, and 6 demonstrate the geometry of the Twin Jet Water Facility.

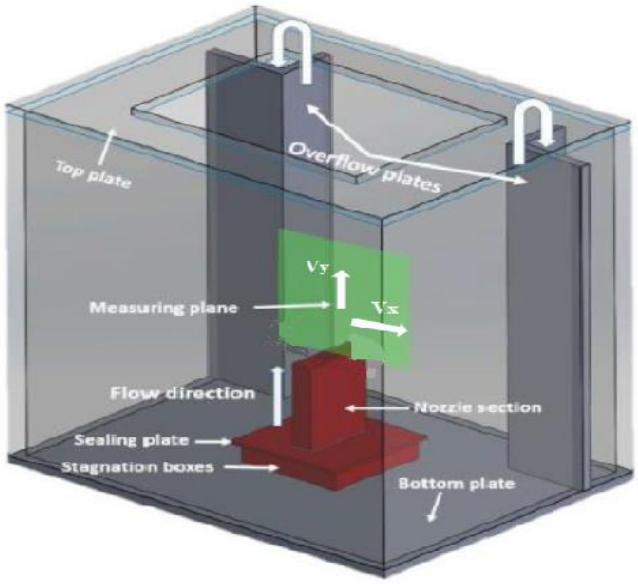

Figure 4: Facility Tank is Shown Along With the Measuring Plane on Which the Experimental and CFD Data Are Extracted.

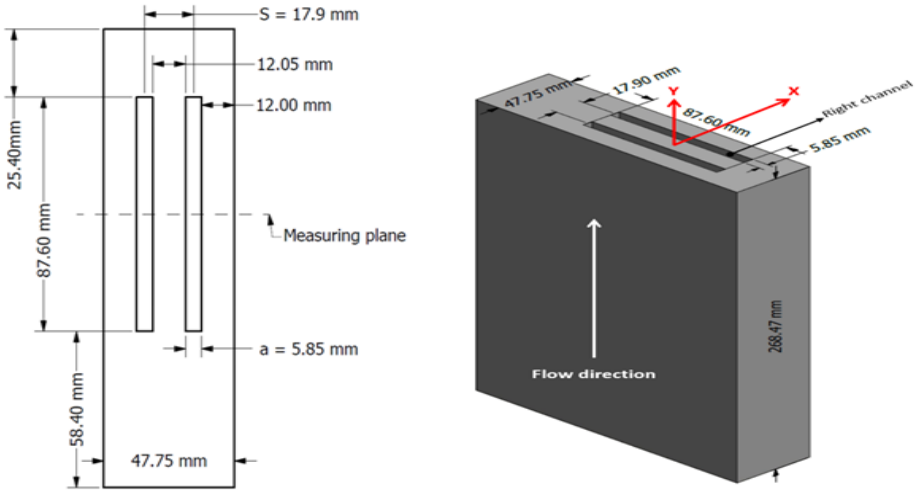

Figure 5: Nozzle Dimensions.

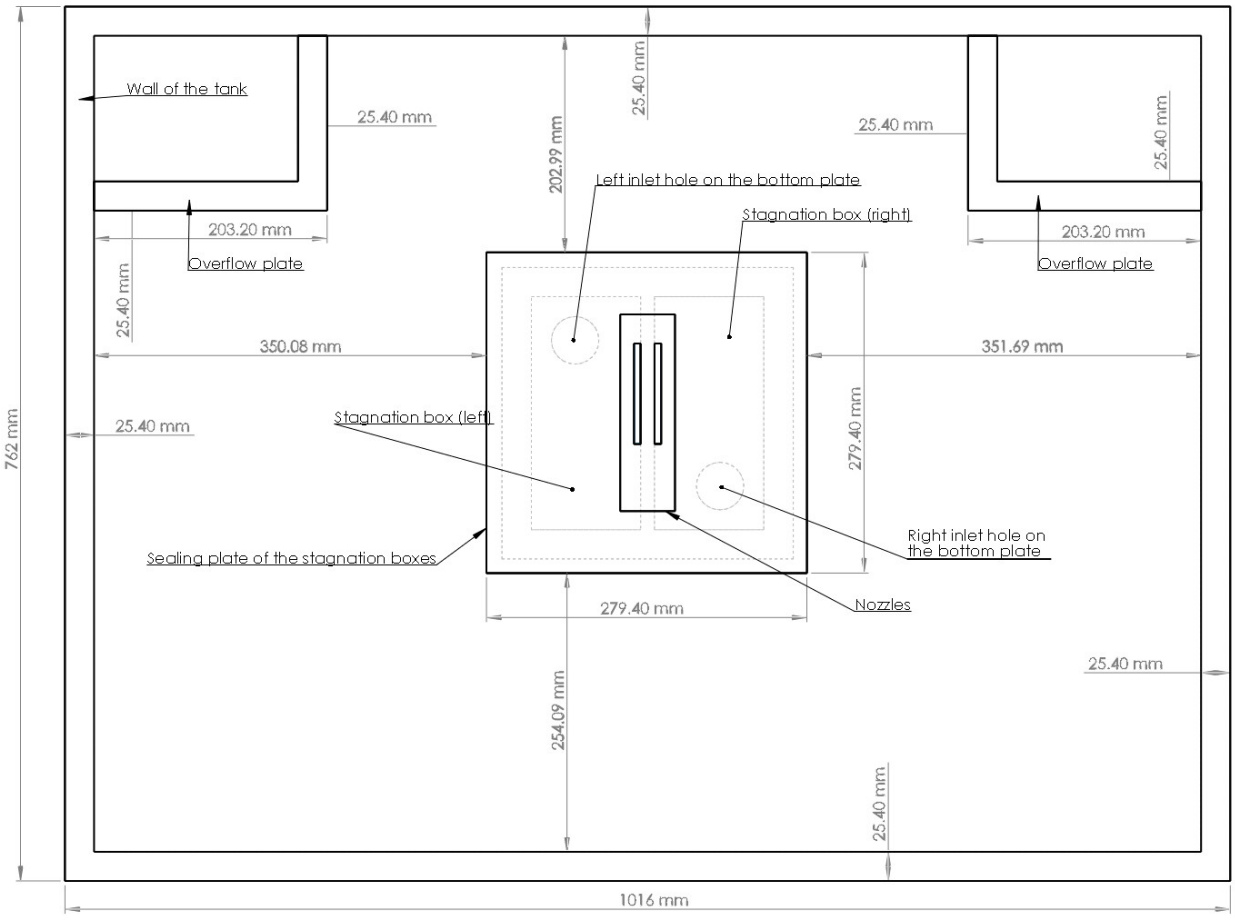

Figure 6: A Top View of the Tank Along With the Corresponding Dimensions.

6. COMPUTATIONAL FLUID DYNAMICS CODE (STARCCM+)

This section is dedicated to demonstrate the software used for the simulation, CD-adapco's STAR-CCM+. STAR-CCM+ is a commercial computer-aided engineering package developed by CD-adapco. Originally developed for computational; fluid dynamics (CFD) simulations, it has been expanded to include additional continuum mechanics models, most notably heat transfer and solid stress models. STAR-CCM+ provides a comprehensive engineering physics simulation package. [4]

STAR-CCM+ uses the finite volume method in it solutions, the solution is subdivided into a finite number of small control volumes, corresponding to the cells of a computational grid. Discrete versions of the integral form of the conservation equations are applied to each control volume. The objective is to obtain a set of linear algebraic equations, with the total number of unknowns in each equation system corresponding to the number of cells in the grid. The dependent variable values are at the cell center, this means that STAR-CCM+ uses a co-located variable arrangement.

Discretization Methods

The finite-volume method transforms the mathematical model into a system of algebraic equations. This transformation involves discretizing the governing equations in space and time. The resulting linear equations are then solved with an algebraic multigrid solver. For unsteady problems, the physical time interval to be analyzed is subdivided into an arbitrary number of sub-intervals that are called time-steps.

General Transport Equation

When the appropriate constitutive relations are introduced into the conservation equations a closed set of equations is obtained. These equations are represented by a generic transport equation. These equations can be integrated over a control volume V and by applying Gauss's divergence theorem, the integral form of the transport equation:

$$\frac{d}{dt}\int_V \rho\phi dV + \int_A \rho v\phi . da = \int_A \Gamma\nabla\phi da + \int_V S\phi dV \ldots (1)$$

Where ϕ represents the transport of a scalar property, A is the surface area of the control volume and da denotes the surface vector. ρ, Γ, and v, are the density, diffusion coefficient and velocity. By selecting appropriate values for the diffusion coefficient Γ and source terms, special forms for the partial differential equations for mass, momentum, energy, and species conservation are obtained.

The four terms in equation (1) starting with the first term on the left hand side are:

1- The transient term, which represents the rate of change of fluid property ϕ inside the control volume with respect to time.
2- The convective flux, which expresses the net rate of decrease of fluid property ϕ across the control volume boundaries due to convection.
3- The diffusive flux, which corresponds to the net rate of increase of fluid property ϕ across the boundaries of the control volume due to diffusion.
4- The source term, which expresses the generation/ destruction of fluid property ϕ within the control volume.

Convective Flux

The discretized convective term at a face can be rearranged as follows:

$$(\phi\ \rho\ v.a)_f = (\dot{m}\phi)_f = \dot{m}_f\phi_f \ldots (2)$$

Where $\dot{m}_f$ is the mass flow rate at the face. The manner in which the fluid property face value ϕ_f is computed from the cell values has a significant effect on the stability and accuracy of the numerical scheme.

Diffusive Flux

The diffusive flux in through internal cell faces of a cell is discretized as:

$$D_f = (\Gamma\nabla\phi.a)_f \ldots (3)$$

Where Γ is the face diffusivity, $\nabla\phi$ is the gradient of fluid property ϕ, and a is the surface area vector.

Gradients

Variable gradients are required at cell centers and at cell-face centers for:

1- Construction of variable values at the cell faces.

2- Secondary gradients calculation for diffusion terms.

3- Pressure gradients calculation for pressure- velocity coupling.

4- Strain-rate and rotation-rate calculations for turbulence models.

In STAR-CCM+, the steps that are involved in the calculation of gradients are:

1- Computing the (unlimited) reconstruction gradients. Here, unlimited means that the gradients do not prohibit the reconstructed field variables on the cell faces from exceeding the minimum and maximum values of the neighboring cells.
2- Limiting the reconstruction gradients. The limited reconstruction gradients. The limited reconstruction gradients are used to determine scalar values at the cell faces. These scalar values are used in computing flux integrals.
3- Computing the cell gradients from the limited reconstruction gradients. This step is only required for the Green-Gauss method. For the Hybrid Gauss-LSQ method, the unlimited LSQ-based gradients are linear-exact and are used as cell gradients in the diffusive fluxes. This approach is more accurate for cell calculations than the Green-Gauss method.

Segregated Flow Solver

The segregated flow solver solves the integral conservation equations of mass and momentum in a sequential manner, they are uncoupled. The non-linear governing equations are solved iteratively one after the other for the solution variables such as velocity components and pressure.

The segregated solver employs a pressure-velocity coupling algorithm where the mass conservation constraint on the velocity field is fulfilled by solving a pressure-correction equation. The pressure-correction equation is constructed from the continuity equation and the momentum equations such that a predicted velocity field satisfies the

continuity equation, which is achieved by correcting the pressure. This method is also called a predictor-corrector approach. Pressure as a variable is obtained from the pressure-correction equation.

STAR-CCM+ implements two pressure-velocity coupling algorithms:

1- SIMPLE

2- PISO

Algebraic Multigrid

Conventional iterative solution algorithms such as Jacobi, Gauss-Seidel, or ILU (Incomplete Lower-Upper) converge much slower with increasing mesh sizes. This slow convergence turn leads to a quadratic increase in computational time. To accelerate solver convergence, STAR-CCM+ employs the Algebraic Multigrid (AMG) method. The concept of multigrid methods is based on the fact that an iterative solution algorithm reduces efficiently the numerical error components whose wave lengths correspond to the cells size (high-frequency errors). The long-wavelength (low-frequency) errors are reduced rather slowly with this method.

Multigrid algorithms apply the following steps:

1- Agglomerate cells to form coarse grid levels.

2- Transfer the residual from a fine level to a coarser level (known as restriction).

3- Transfer the correction from a coarse level back to a finer level (known as prolongation).

7. SIMULATION

This geometry was constructed using Auto Inventor software package. The geometry is shown in Figure 7. The red points are monitors that were used to monitor quantities such as temperature and velocity to ensure convergence and to compare between different size meshes. The line above the nozzles outlets is a line probe used to monitor the streamwise velocity of the flow and it was compared between the three mesh sizes used.

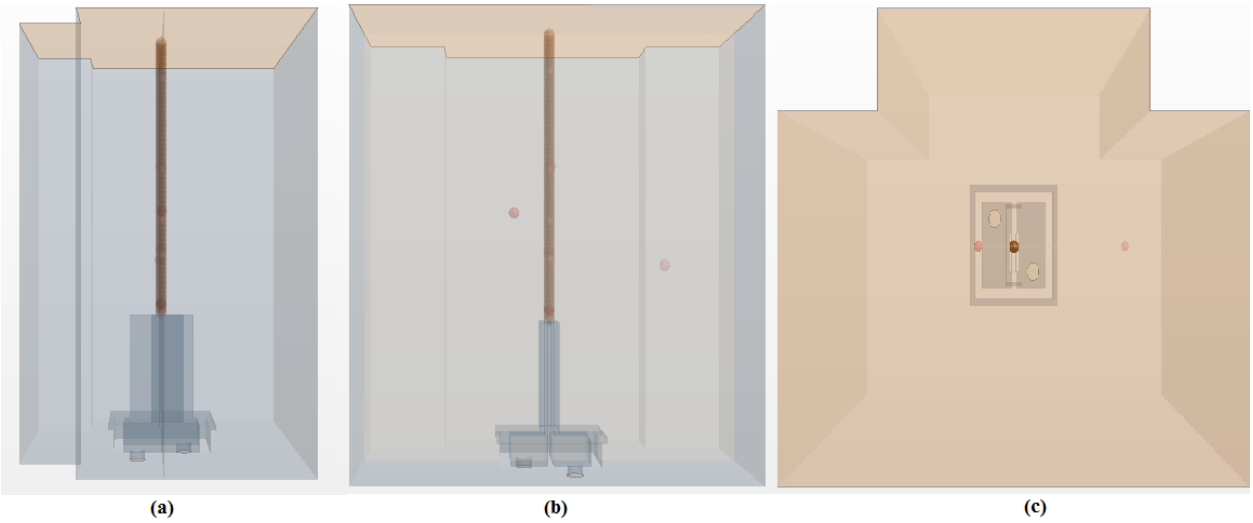

Figure 7: Geometry of the Simulation Shown from Different Angles. a) Side View. b) Front View. c) Top View.

The two circular cylinders beneath the stagnation box were designated as inlets for the simulation. The overflow plates are shown in the geometry, but were not modeled. Instead the top surface of the tank was chosen to be a pressure outlet. The walls were modeled as no slip boundaries. Three cases were run for this project; steady Iso-thermal and steady Non-Isothermal. The Parameters for the simulation are shown in Table1.

Table 1: Simulation Parameters Used As Boundary Conditions.

Paramters	Steady Iso	Steady- Non Iso
Mass Flow Rate Kg/s	0.378	0.378
Left NozzleTemperature / °C	-	65.5
Right NozzleTemperature / °C	-	24.3

The Turbulence Intensity was around 5%. The length scale for turbulence was around 0.07 of the hydraulic diameter of the nozzles.

8. MESH

STAR-CCM+ contains different types of meshing models that can be used to generate a volume mesh starting from a suitably prepared surface. The Trimmer mesh is volumetric mesh that generates a volume mesh by cutting a hexahedral template mesh with geometry surface. The trimmer mesh is used as it offered better mesh quality properties than the generated polyhedral mesh, such angle skewness and cell quality. To assist in capturing high velocity gradients volumetric controls where used. Volumetric controls are shapes which allow us to increase the meshing density within the volume of these shapes. Two volumes were used; a cone and rectangle, these are called volume control 1 and 2, respectively. The base size of these controls and base size of each mesh is shown in Table 2. The mesh configuration is shown Figure 8.

Table 2: Mesh Sizes of the Three Meshes Used.

Mesh	Base Size/m	Volume Control 1	Volume Control 2	Number of Cells-Million
Coarse Mesh	**0.00500**	**0.00400**	**0.003500**	**5.78**
Fine Mesh	**0.00384**	**0.00307**	**0.002688**	**11.87**
Finest Mesh	**0.00295**	**0.00236**	**0.002065**	**19.45**

To ensure the independence of the simulation results from the mesh size, a mesh dependence study was carried out. The streamwise velocity was monitored for all mesh

sizes; coarse, fine, and finest and is plotted in Figure 9. Six monitors for velocity and temperature, were used in the simulation, and minor differences were noted for values between the fine and the finest mesh. For the results shown in this document, the finest mesh was used.

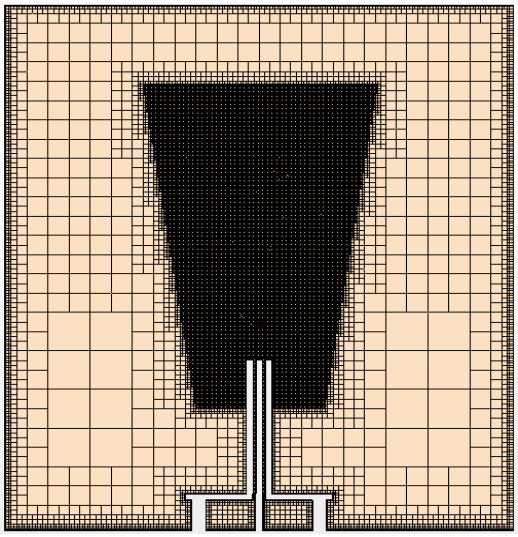

Figure 8: Trimmer mMesh Generated for the Geometry Along With Volumetric Controls.

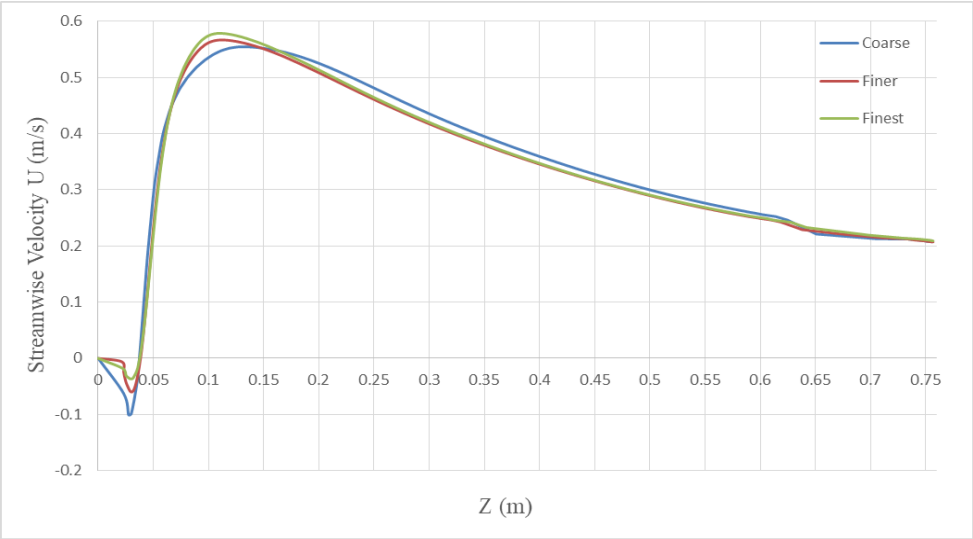

Figure 9: Mesh Sensitivity Results for Three Mesh Sizes.

9. TURBULENCE MODEL – STANDARD K-ε

The κ-ε model is one of the most common turbulence models. This is model is a two equation model. Two equation models, like κ-ε and κ-ω are used in most engineering problems. Two equation models carry their name from the fact that these models include two extra transport equations to represent the turbulent properties of the flow. This permits the model to carry the effects from the history of the flow, such as convection and diffusion of turbulent energy.

In the κ-ε model the transported variables are the κ, the turbulent kinetic energy, and ε the turbulent dissipation rate. The turbulent kinetic energy and the turbulent dissipation determine the energy of the turbulence, and the turbulent dissipation determines the scale.

One of the basic assumptions of the of two equation models is the Boussinesq assumption, which states that the Reynolds stress tensor, τ_{ij} is proportional to the mean strain rate tensor,S_{ij} , and is written:

$$\tau_{ij} = 2\mu_t S_{ij} - \frac{2}{3}\rho k \delta_{ij} \ldots(4)$$

Where, μ_t is the eddy viscosity, which is a scalar property that is computed from the two transported variables. The last term is included for modeling incompressible flow to ensure that the definition of turbulence kinetic energy is obeyed.

$$\kappa = \frac{\overline{u_i' u_i'}}{2} \ldots (5)$$

Where u' is the root-mean-square of the turbulent velocity fluctuations and U is the Reynolds averaged mean velocity. The same equation can be written as:

$$-\rho\overline{u_i' u_i'} = \mu_t \left(\frac{\sigma U_i}{\sigma x_j} + \frac{\sigma U_j}{\sigma x_i}\right) - \frac{2}{3}\rho\kappa\delta_{ij} \ldots (6)$$

The Boussinesq assumption provides a huge simplification which allows one to think of the effect of turbulence on the mean flow in the same way as molecular viscosity affects a laminar flow. Unfortunately, the Boussinesq assumption is not always valid as there is nothing that nictitates the Reynolds stress tensor must be proportional to the strain rate tensor [5]. The turbulence model used for this simulation is the standard κ-ε model.

For turbulent kinetic energy κ:

$$\frac{\partial}{\partial t}(\rho\kappa) + \frac{\partial}{\partial x_i}(\rho\kappa u_i) = \frac{\partial}{\partial x_j}\left[\left((\mu) + \frac{\mu_t}{\sigma_k}\right)\frac{\partial\kappa}{\partial x_j}\right] - 2\mu_t S_{ij} S_{ij} - \rho\varepsilon \ldots (7)$$

For dissipation ε:

$$\frac{\partial}{\partial t}(\rho\varepsilon) + \frac{\partial}{\partial x_i}(\rho\varepsilon u_i) = \frac{\partial}{\partial x_j}\left[\left((\mu) + \frac{\mu_t}{\sigma_k}\right)\frac{\partial\varepsilon}{\partial x_j}\right] + C_{\varepsilon 1}\frac{\varepsilon}{\kappa}\, 2\mu_t S_{ij} S_{ij} - C_{\varepsilon 2}\rho\frac{\varepsilon^2}{\kappa} \ldots (8)$$

The turbulent viscosity is:

$$\mu_t = \rho C_\mu \frac{\kappa^2}{\varepsilon} \ldots (9)$$

Where,

μ is the viscosity.

ρ is the density of the fluid.

u is the velocity.

S, is the modulus of the mean rate-of-strain tensor.

And $C_{\varepsilon 1}$, $C_{\varepsilon 2}$, C_{μ}, σ_k, and σ_{ε} are constants and are equal to 1.44, 1.92, 0.09, 1.0, and 1.3, respectively. The standard κ-ε model was used for two reasons. First, the standard κ-ε model compared more favorably with experimental data [6]. Second, the software package used, STAR-CCM+ has the buoyancy terms built into the κ-ε models only. Also, several studies have studied jet behavior (turbulent shear flow) and compared different turbulence models, and have found that κ-ε model family provides very good predictions compared to other models. [7][8]

10. RESULTS

This section is dedicated to present the result of the simulation. The quantities of interest that were plotted and compared were, the UV Reynold stress component, the streamwise velocity, the lateral velocity, and the vorticity. The quantities were plotted and compared for both the steady state runs, the Non-Isothermal case (Non-Iso) and the Isothermal case (Iso). The quantities of interest were plotted at three different non-dimensional heights, Y/a = 1.4, 4.2, and 7.0. The results are shown in the following figures.

10.1 Y/a = 1.7

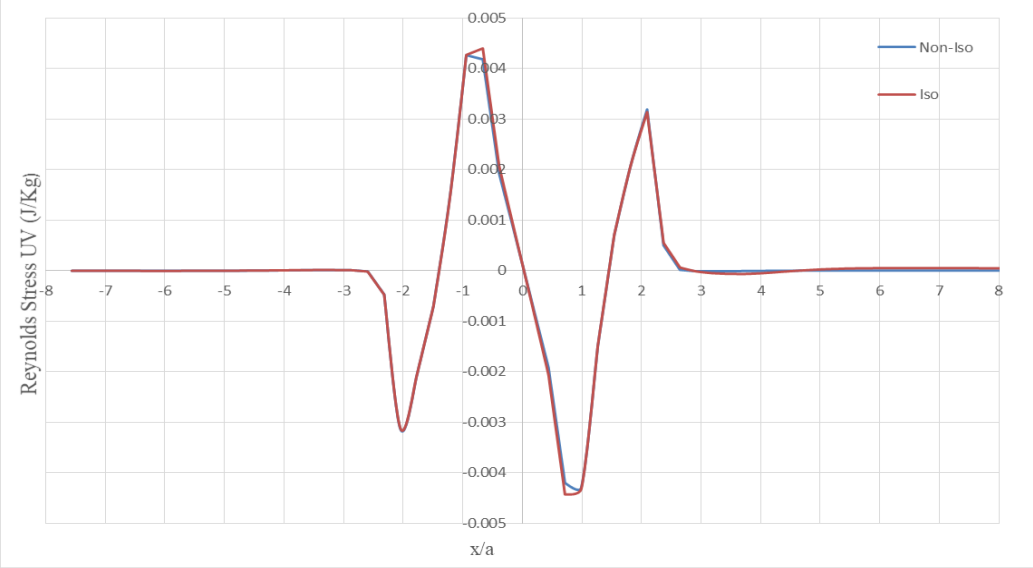

Figure 10: UV Component at Y/a= 1.7.

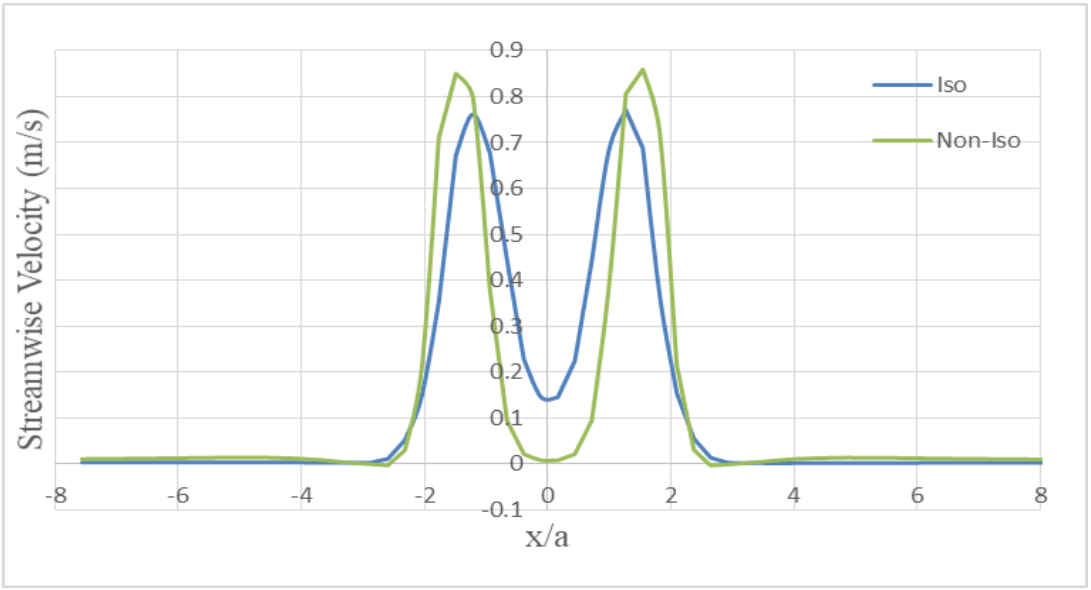

Figure 11: Streamwise Velocity at Y/a = 1.7.

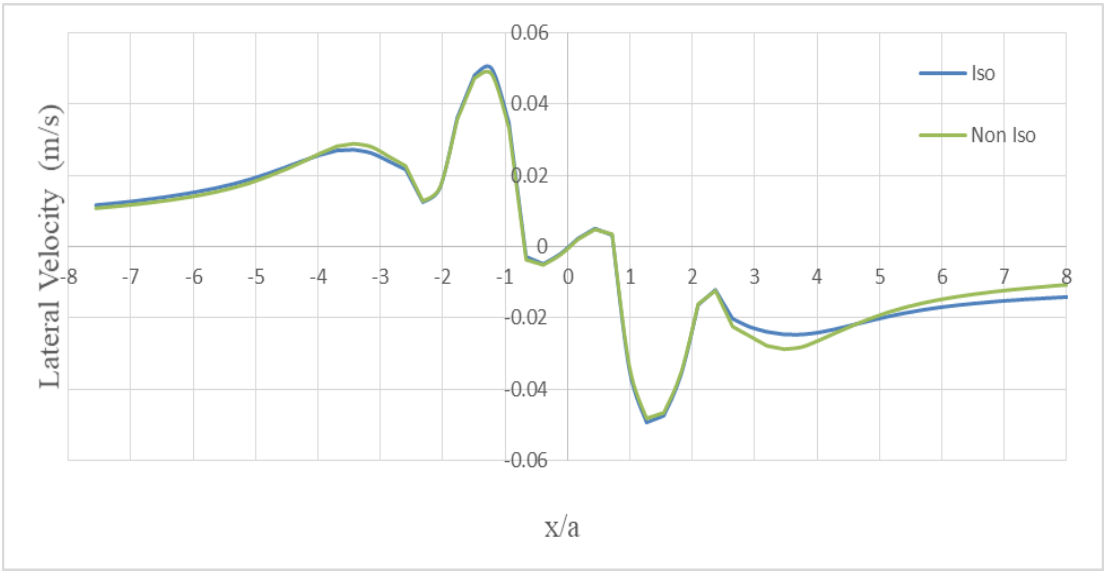

Figure 12: Lateral Velocity at Y/a= 1.7.

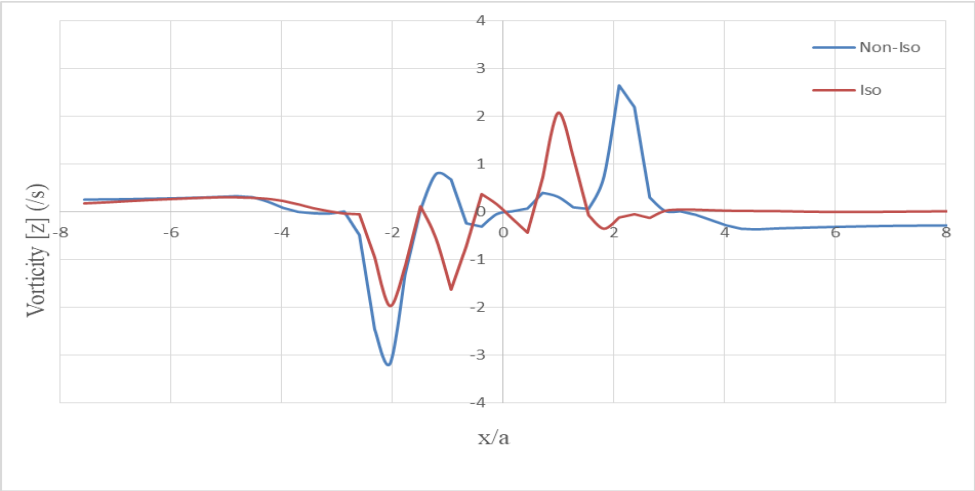

Figure 13: Streamwise Vorticity at Y/a = 1.7.

10.2 Y/a = 4.2

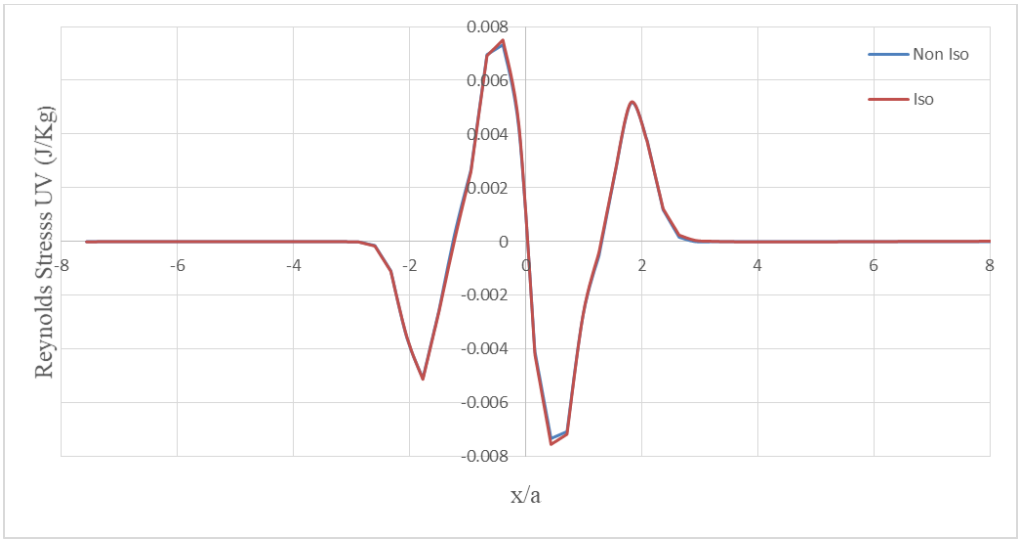

Figure 14: The UV Component at Y/a= 4.2.

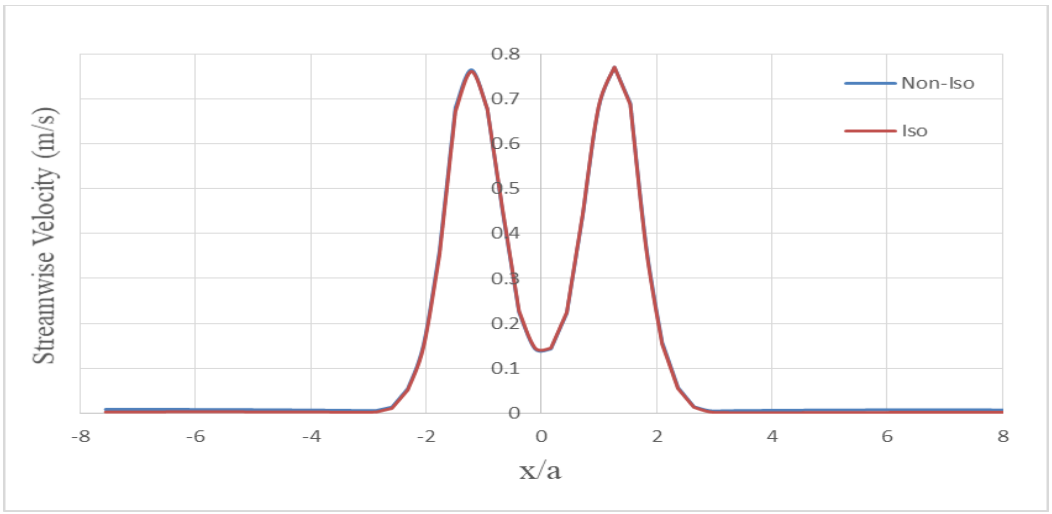

Figure 15: Streamwise Velocity at Y/a = 4.2.

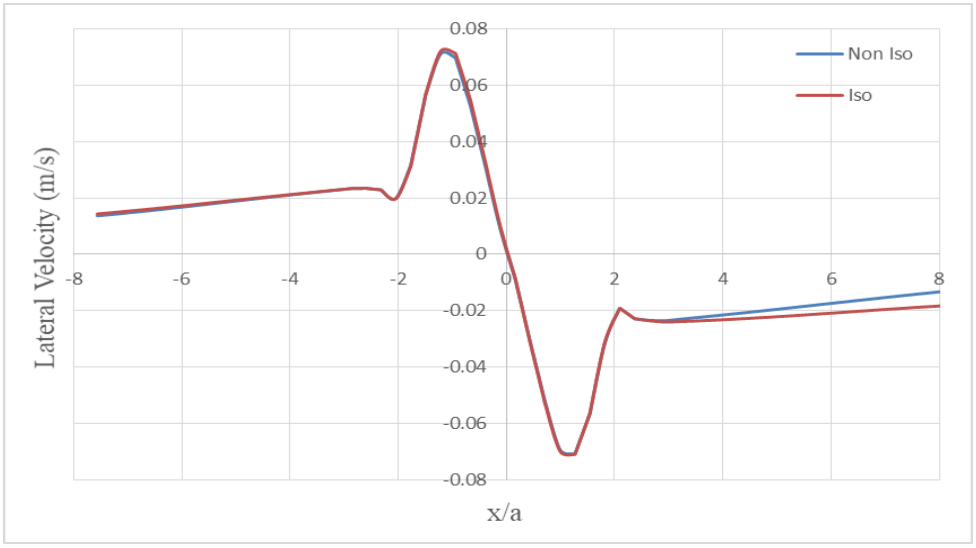

Figure 16: Lateral Velocity at Y/a= 4.2.

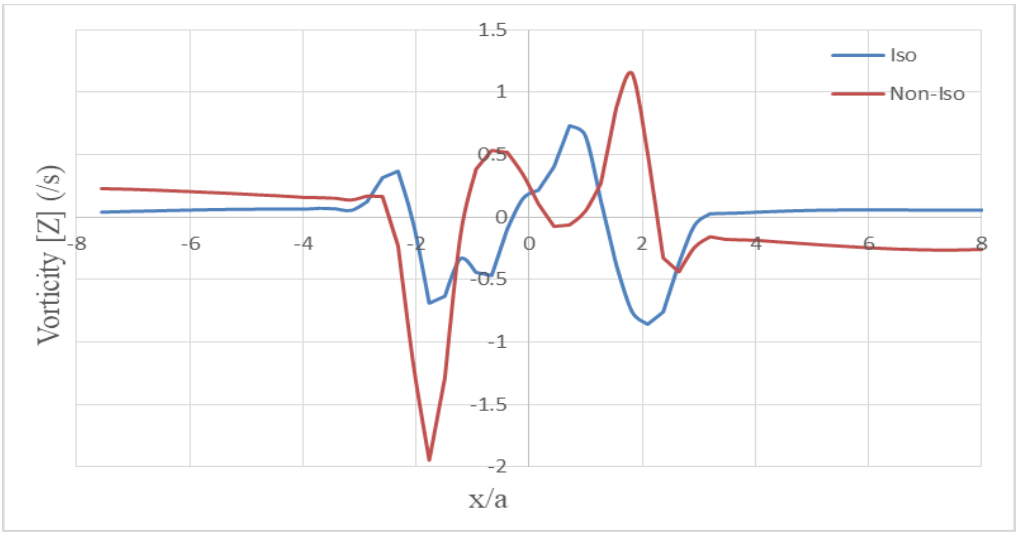

Figure 17: Streamwise Vorticity at Y/a = 4.2.

10.3 Y/a = 7.0

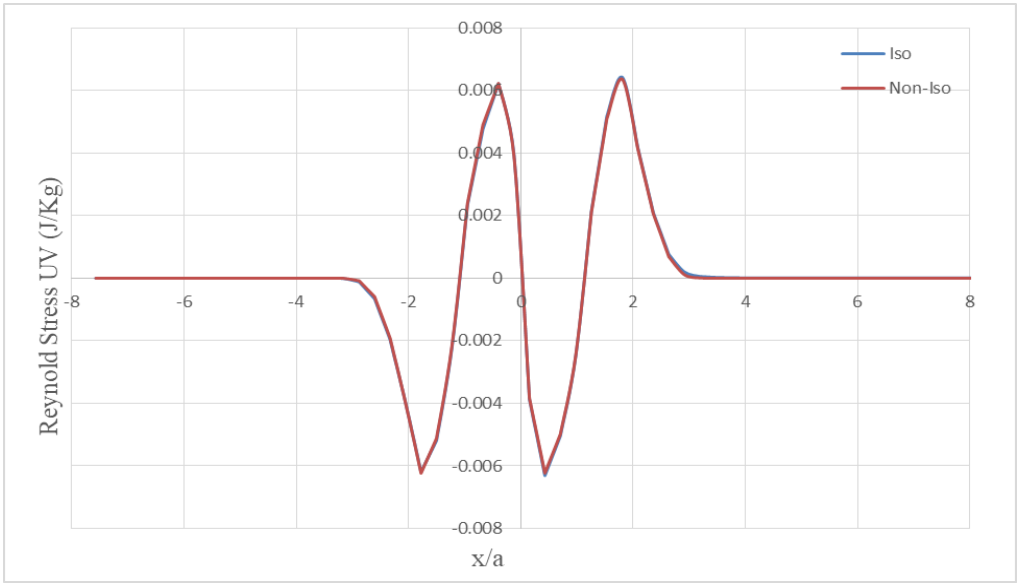

Figure 18: UV Component at Y/a= 7.0.

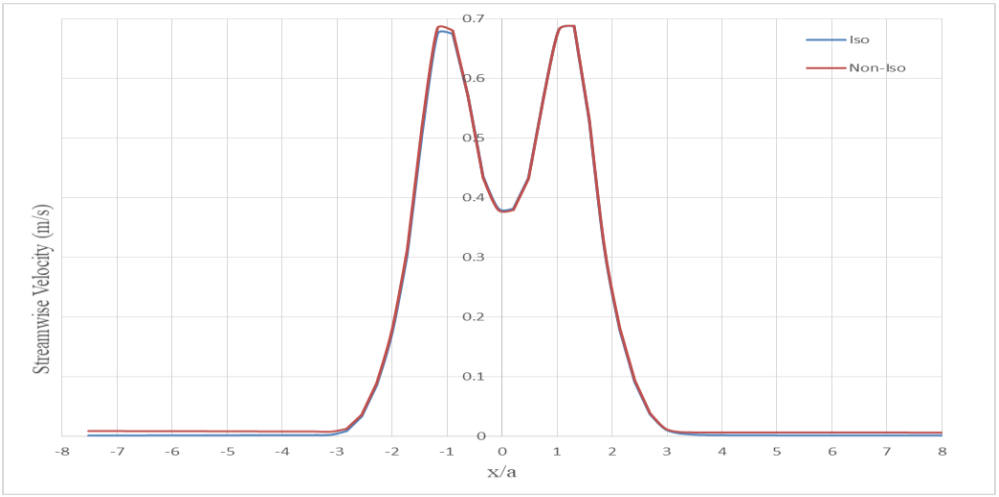

Figure 19: Streamwise Velocity at Y/a = 7.0.

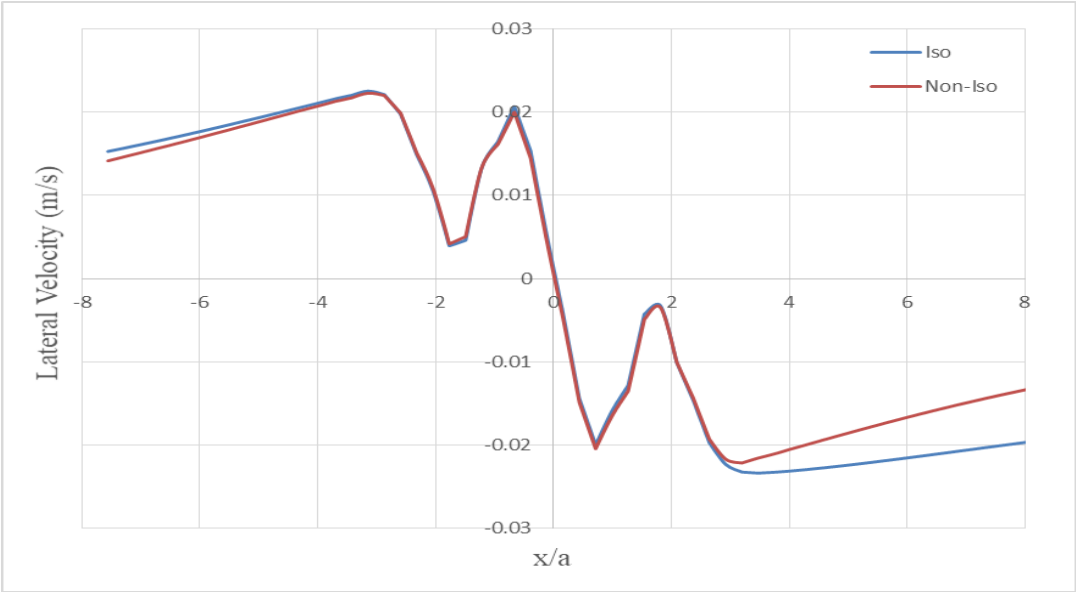

Figure 20: Lateral Velocity at Y/a= 7.0.

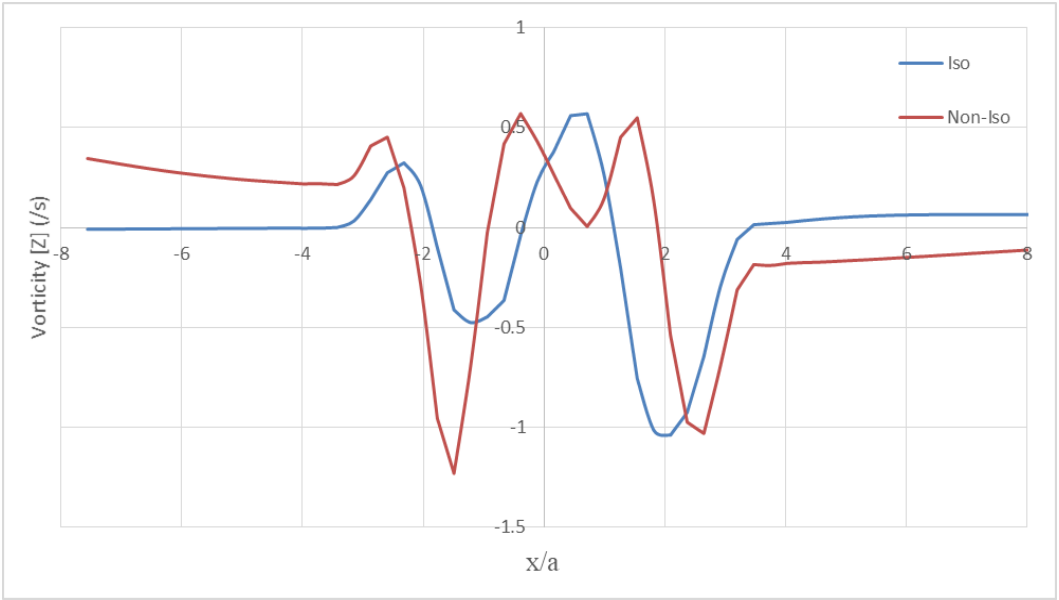

Figure 21: Streamwise Vorticity at Y/a = 7.0.

11. CONCLUSIONS

The Isothermal and Non-Isothermal twin jets have been studied and analyzed. The two jets had equal velocities and temperatures in the isothermal case, and equal velocities and different temperatures in the non-isothermal case. The effect of temperature difference will induce buoyancy effects, which could not be perfectly modeled in steady state analysis. Another factor to consider is that, in the non-isothermal case, the temperature difference, and hence, the density difference percentage is small, this will affect the amount of buoyancy produced, that it would not be accurately captured in a RANS model. Both cases show different vorticities. Vorticity, which is an indication of the rotation speed of the fluid particles in the x-y plane for plots, is also an indication of enhanced mixing as the friction forces between the moving jets and the static surrounding have generated these vortices. Vorticity is an indication of mixing, and the fact that the results show different vorticity values for the non-isothermal case shows that the temperature difference in the jets affected their mixing. There is a small difference in the lateral velocity of the jets which reflects upon high entrainment in the non-isothermal case. The Reynold stresses seem to be equal for both cases, this can be due to the inaccuracies associated with RANS models and their deficiency in capturing some scales of physics. This drawback can be overcome by using a Large Eddy Simulation (LES) that will be able to resolve more physics and thus provide more insight on the underlying phenomena. For future work, different turbulence models will be used and compared.

REFERENCES

[1] E. Tanaka, 1974. "The Interference of Two Dimensional Parallel Jets (1st Report, Experiments on Dual Jets)", *Bull. JSME*, 13(56), pp. 272-280.

[2] E. Tanaka 1974, "The Interference Of Two-Dimensional Parallel Jets (2nd Report, Experiments On The Combined Flow Of Dual Jet", *Bull. JSME*, 17(109), pp. 920-927.

[3] H. Wang, S. Lee, Y. A. Hassan, Arthur E. Ruggles. 2015, "Laser-Doppler measurements of the turbulent mixing of two rectangular water jets impinging on a stationary pool", *International Journal of Heat and Mass Transfer*.

[4] Siemens, STAR-CCM++ v12.02.010 User's Guide.

[5] D.C. Wilcox, (1993), Turbulence Modeling for CFD, *DCW Industries, Inc.*

[6] S. Suyambazhahan, T. Sundararajan, S. K. Das, 2004, "Numerical Simulation of Flow and Thermal Oscillations in Non-Isothermal Turbulent Multiple Jets", *ASME Heat and Mass Transfer Conference.*

[7] S. Suyambazhahan, T. Sundararajan, Sarit K. Das, 2007, "Numerical Study of Flow and Thermal Oscillations in Buoyant Twin Jets", *International Communications in Heat and Mass Transfer.*

[8] J. C. S. Lai, A. Nasr, 1998, "Two Parallel Plane Jets: Comparison of the Performance of Three Turbulence Models", *Institution of Mechanical Engineers.*

SUPPLEMENTAL SOURCES CONSULTED

[9] S.B. Pope, 2000, Turbulent Flows, *Cambridge University Press.*

[10] S. V. Patankar, 1980, "Numerical Heat Transfer and Fluid Flow", *Taylor and Francis.*

[11] H. W. Liepmann, J. Laufer, 1947, "Investigations of Turbulent Mixing", *National Advisory Committee for Aeronautics*, Washington, D.C., No. 1257.

[12] J. H. Ferziger, M. Peric, 2002, "Computational Methods for Fluid Dynamics", *Springer.*

[13] A.A. Townsend, F.R.S. 1976, "The Structure of Turbulent Shear Flows", *Cambridge University Press.*

[14] Peter Davidson, 2015, "Turbulence an Introduction for Scientists and Engineers", *Oxford University Press.*

[15] H. Li, H. Wang, Y. A. Hassan, N. K. Anand, 2016, "Computational Fluid Dynamics Analysis of Two Parallel Rectangular Jets Using OPENFOAM", *ICONE24-61046.*